

# Selection and Ranking of Brain Tumor MRI Image Features

Ameen Mohammed Abd-Alsalam Selami

Kirkuk University/ College of Engineering – Electrical Engineering Dept. Iraq

---

## ABSTRACT

This paper presents a study about the features that are taken from abnormal (cancerous) brain MRI images, and how these features differ in value between the normal and the abnormal segments of the brain MRI images. The proposed algorithm depends on gathering abnormal brain MRI (axial view) images, applying some preprocessing as: Removing unnecessary portions, Normalizing sizes, Enhancing images through filters then dividing the image into small normal and abnormal sub segments with a size of 32 by 32 pixels ready to be feature extracted. In this paper 15 image features are extracted and studied to decide and classify the normal and abnormal sub segments and also to select the most effecting features and finally to rank them. The types of the features are: Histogram, Transform, Texture, and Statistical features. These features are leveled to 3 levels: Low, Medium, and High as (L, M, H) according to their values and are calculated in normal and abnormal sub segments to make a statistical study about their existence in both normal and abnormal sub segments. A total of 69 abnormal MRI images were taken from 11 ill persons, containing 444 normal and 345 abnormal sub segments, making a total of 789 sub segments to be feature extracted and studied. The paper shows that the features of (mean, variance, standard deviation, entropy, vertical, energy, homogeneity, kurtosis, mode and RMS roughness) were affected by the existence of tumors, while the features (horizontal, diagonal, contrast, correlation, skewness) had no effect.

**Keywords:** MRI, Brain Tumor, Image Features, Segmentation, Histogram, Transform, Texture.

---

## 1. INTRODUCTION

According to World Health Organization, tumor is considered one of the most common brain diseases, and it is a reason for the top-ten mortalities over the world nowadays. So it is required to make an accurate and early diagnosing to reduce the danger of brain tumors and save lives [1]. The tumor that forms in the brain is considered an abnormal mass of tissue in which some cells grow in an unregulated shape. Brain space is taken by the growth of a tumor within the skull causing damage by increasing pressure in the brain, shifting the brain or pushing against the skull, and by invading and damaging nerves and healthy brain tissues [2]. From all the methods and devices used to detect brain tumors, the Magnetic Resonance Imaging (MRI) is the common and preferred one to be used. The MRI is a method used to visualize pathological or other physiological alterations of living tissues. It is commonly used for brain tumor imaging because of the following reasons [3]:

1. It does not use ionizing radiation like Computed Tomography (CT), Single Photon Emission Computed Tomography (SPECT) and Positron Emission Tomography (PET).
2. Its contrast resolution is higher than the other techniques mentioned above.
3. It is able to generate 3D space images which enable it to have superior tumor localization.
4. Its ability in the acquisition of both functional and anatomical information about the tumor during the same scan.

Classifying brain MRI images to normal and abnormal images depending on some image features is necessary to differentiate the normal images from the pathological ones. This could be done using different classification techniques and algorithms in which some of them may use hybrid techniques too [4]. So the abnormal classified images need to be segmented to normal and abnormal segments within the abnormal MRI image to calculate the tumors size and find its position [5]. It is very important to be accurate and precise in detecting abnormal MRI images, calculating the tumor size, and selecting its position, because these steps are considered the diagnosing steps and are going to be followed by the surgical intrusion. Therefore in this paper 15 different types of features are being studied statistically through noticing the

variation in their values. This gives an indication about the existence of the tumor. Analyzing results should help in selecting the effective features and ranking them. These features are gathered from small, sub segments of both normal and affected portions in the same abnormal MRI image.

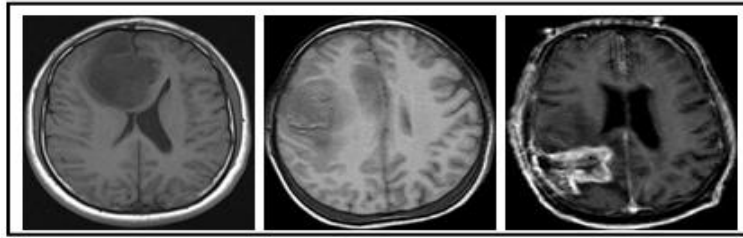


Figure 1: Samples of brains MRI images - Axial View

## 2. RELATED WORKS

There were several attempts to classify MRI images into normal and abnormal images, then using some segmentation techniques to isolate the affected portions from the normal portions within the same abnormal MRI image. Some of these works are: A Ph.D. thesis prepared by Zhang Nan [6] shows that using multi-kernel support vector machine (SVM), is one of the ways to the classify a human brain in MRI images, the author determines that an adaptive training should be designed to follow-up the changes of tumors during several MRI examinations. After a year, a new method depending on the neural network is used to classify brain tumors [7]. In the same year S. Javeed Hussain, T. Satya Savithri, and P.V. Sree Devi [8] developed a classification and a segmentation process of the MRI images using some histogram and transform image features as inputs for the Fuzzy Inference System (FIS) and FFBNN. The author D. K. Kole et. al., in [9] use genetic algorithm based clustering techniques and region growing techniques to detect brain tumors and isolate its cells in MRI images. Texture features were also used for classification and segmentation purpose in several works [10, 11, 12]. These works show the effectiveness of texture features in characterizing brain tumor tissues in MRI. In addition to the textural image features, Seeded Region Growing Method is a segmentation technique used by M. Kumar and K. K. Mehta to apply segmentation on MRI images that contain tumors [13]. According to N. Just [14], Metrics such as kurtosis and skewness (which are also histogram features), demonstrated to be strong and reliable quantitative surrogate markers of tumor heterogeneity with a more direct correlation to the underlying structural, physiological, molecular as well as metabolic changes occurring upon tumor progression with and without therapy. Adegoke, B.O, Ola, B.O. and Omotayo, M.E end up with a conclusion says that screening, ranking and selecting of features should be done for any medical image processing decisions [15].

Saurabh Shah and N.C. Chauhan suggest using Gabor filters to extract texture features from MRI images and perform a classification based on SVM, also they suggest comparing the histograms of the two halves of the brain to find the ROI which is being used to extract features from and use ANN for classification [16]. Although the study is about lung cancer detection, but R. Kishore confirms that screening, ranking and selecting of image features should be considered after extracting the features that to be analyzed [17]. Recently in [18], V Sheejakumari and Sankara Gomathi show that some histogram, shape and texture features could be used for brain tumor detection and segmentation with the help of a modified neural network. In [19], the features of Area, Entropy, Contrast and Homogeneity were used by K. Muthukarpagam et al. to detect brain tumors in MRI images.

## 3. PROPOSED METHOD:

Most of the previous works use K-means, Otsu, Seeded Region Growing and other clustering and segmentation techniques, but in this paper the work focuses on getting the feature values of the small segments within the abnormal MRI images, in attempt to select and isolate the affected sub segments according to the change in the feature values, so if the affected sub segments are detected, then they could be gathered and segmented as a whole one segment easily. This will help the idea of selecting and ranking the effective features in brain MRI images. Thus the major stages of the proposed method are:

- 1- **Preprocessing**, which contains:
  - Gathering brain MRI images and selecting the abnormal images.
  - Removing unnecessary information (if there is any).
  - Normalizing sizes.
  - Removing noise.
- 2- **Dividing the images into small sub segments of 32 by 32 pixels.**

- 3- Features extraction from the sub segments.
- 4- Dividing the features into 3 levels (L, M, H), and studying their variations in normal and abnormal sub segments.
- 5- Making conclusions about the effective features that should be depended in future works.

### Preprocessing

Gathering MRI images of pathological brains is the first thing to do. These images could be gathered from different sources like local hospitals or from specialized web sites. The web site: <http://www.med.harvard.edu/AANLIB/home.html> is a good source of data set belonging to Harvard Medical School. Then selecting the abnormal images to apply the preprocessing steps is performed.

It is necessary to remove any unrelated and unimportant information from these images like the name and the age of the patient, the scanning date of the image and any other related information if exist. Also the large area of the black background is not preferred. It is not allowed for this information to appear neither while dividing the images into small 32 \* 32 pixels nor while features extracting because they are not involved in the processes later.

In order to apply an automated process to all images, all the images should be equal in their size. This step is known as size normalization. In this paper they are all normalized to 256 \* 256 pixels automatically.

Finally, removing any contained noise is necessary to make the images ready for the next step of processing. According to [18] and [19] the median filter is the most accurate filter to be used to enhance MRI images against the noise that may exist. Therefore median filter is used followed by histogram equalization which is used to enhance the contrast.

### Dividing the Images into Small Sub Segments of 32 by 32 Pixels

The MRI images gathered are in the size of 256 by 256 pixels. The proposed technique considers dividing the images to small sub segments, 64 blocks of 32 by 32 pixels, the smallest tumor or abnormality could be involved in a sub segment, thus the sub segments features may change in value in case of holding a tumor. Studying the features of a small segment in both cases makes it easy to differentiate between normal and pathological segments within the abnormal MRI image. Another advantage of dividing the images to small segments is to ignore the borders of the image that contains the skull and portions of the black background which is free of normal and abnormal tissues and studying its features may result in faulty results.

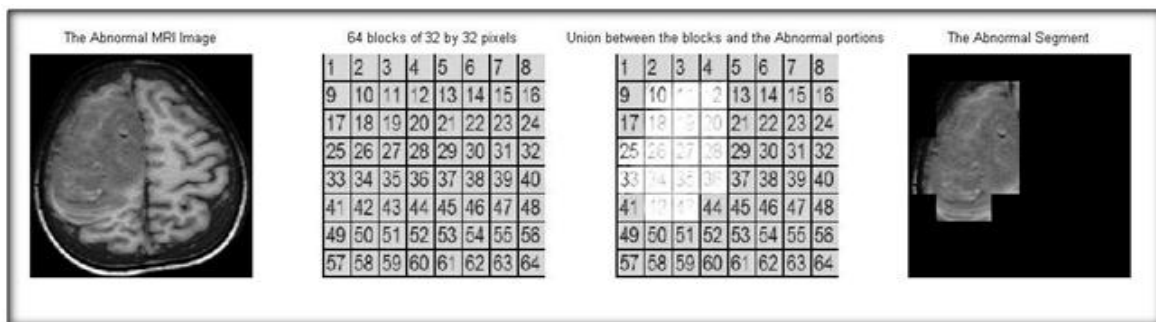


Figure 2: Dividing the MRI image to 32 by 32 Blocks

### Features Extraction from the Sub Segments

Most of the studies on the medical images depend on extracting different types of features from the medical images, as well as in this paper, the features could be divided into four types:

- 1- Histogram Features: The Mean Value, Variance, Standard Deviation, Entropy, Skewness, Kurtosis and the RMS Roughness features.
- 2- Transform Features: Horizontal, Vertical and Diagonal.
- 3- Texture Features: Contrast, Correlation, Homogeneity and Energy.
- 4- Statistical Features: The Mode value.

**Histogram Features [20]:**

Histogram features are used to represent the out-looking properties of pixels within the image. The mean value is one of the basic features which could be represented as below:

$$M_s = \frac{1}{N * M} \sum_{i=1}^M \sum_{j=1}^N z(i, j) \dots\dots\dots (1)$$

Beside the mean value, there are two features could be extracted directly from the image, the Variance and the Standard Deviation, which could be expressed as:

$$\text{Variance } (\sigma^2) = \frac{1}{N * M} \sum_{i=1}^M \sum_{j=1}^N (z(i, j) - M_s)^2 \dots\dots\dots (2)$$

$$\text{The Standard Deviation } (\sigma) = \sqrt{\text{Variance}} \dots\dots\dots (3)$$

Where z (i, j) represents the pixels intensity value in the image, i and j are the pixel positions, N and M are the height and width of the image.

In image processing, the feature of Entropy measures the randomness and disordering of the grey level distribution and its maximum value could be achieved when all elements are equal The P z (i, j) represents the probability of pixels intensities.

$$\text{Entropy} = - \sum_{i=1}^M \sum_{j=1}^N P z(i, j) \text{Log}_2 P z(i, j) \dots\dots\dots (4)$$

Also there is the feature of skewness which is a measure of the lack of symmetry. A distribution, or a data set, is symmetric if it looks the same to the left and right of the center point. On the other hand the feature of Kurtosis is a measure of whether the data are heavy-tailed or light-tailed relative to a normal distribution. That is, data sets with high kurtosis tend to have heavy tails, or outliers while data sets with low kurtosis tend to have light tails, or lack of outliers. The both features are statistical histogram features. To calculate the skewness and the kurtosis, we use the formulas below [21]:

$$\text{Skewness} = \frac{\sum_{i=1}^M \sum_{j=1}^N (z(i, j) - M_s)^3 / M * N}{6^3} \dots\dots\dots (5)$$

The previous formula is referred to as the Fisher-Pearson coefficient of skewness.

$$\text{Kurtosis} = \frac{\sum_{i=1}^M \sum_{j=1}^N (z(i, j) - M_s)^4 / M * N}{6^4} \dots\dots\dots (6)$$

Another feature is the RMS Roughness feature, a statistical parameter that represents the variance of the amplitude distribution function, it could be written as [22]:

$$\text{RMS\_R} = \sqrt{\sum_{i=1}^M \sum_{j=1}^N (z(i, j) - M_s)^2 / N * M} \dots\dots\dots (7)$$

**Transform Features:**

Wavelet transform allows different levels of resolution for images and plays the role of isolating the discontinuities at the image edges, therefore it is considered a good tool to be depended in feature extraction. The Discrete Wavelet Transform (DWT) uses the Haar function, “Haar wavelet” in image coding and edge extraction [23]. The figure shown below represents a two level decomposition of wavelet:

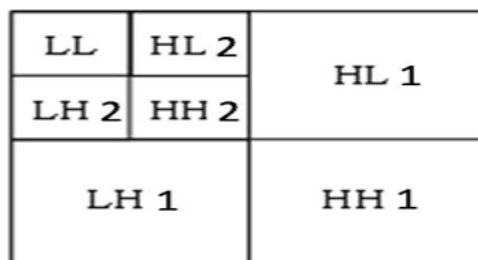


**Figure 3: Structure of Wavelet Decomposition**

The features of (HL, LH and HH) which represent the Horizontal, Vertical and Diagonal, are extracted after applying 2 levels of Haar wavelet to the sub segment images. Their equations are computed as:

$$H = \frac{1}{M N} \sum_{i=1}^M \sum_{j=1}^N h(i, j) \dots\dots\dots (8)$$

$$V = \frac{1}{M N} \sum_{i=1}^M \sum_{j=1}^N v(i, j) \dots\dots\dots (9)$$

$$D = \frac{1}{M N} \sum_{i=1}^M \sum_{j=1}^N d(i, j) \dots\dots\dots (10)$$

The parameters H, V, and D are the coefficients of the horizontal, vertical, and diagonal bands of the image.

**Texture Features [20]:**

The texture features of Gray Level Co-occurrence Matrix (GLCM) are used in this paper, their equations and description are computed as:

$$\text{Correlation} = \sum_i^N \sum_j^N (i - \mu_i) \cdot (j - \mu_j) \cdot Z(i, j) / \sigma_i \sigma_j \dots\dots\dots (11)$$

Where  $\mu_i$  is the Mean Value,  $\sigma_i$  is the Standard Deviation in the rows, and  $\sigma_j$  is the Standard Deviation in the columns of the image. Correlation provides the correlation between 2 pixels in a pixel pair, so it gives an indication of how strong the pixels are correlated together.

$$\text{Homogeneity} = \sum_i^N \sum_j^N Z(i, j) / 1 + |i - j| \dots\dots\dots (12)$$

Homogeneity is a measure of how much pixel pairs are homogeneous. It has a high value in case of having large values in the main diagonal or in the case of similar gray levels of each pixel pairs.

$$\text{Energy} = \sum_i^N \sum_j^N Z^2(i, j) \dots\dots\dots (13)$$

Energy, which is also known as uniformity, it is a measure of the number of repeated pairs.

$$\text{Contrast} = \sum_i^N \sum_j^N (i - j)^2 Z(i, j) \dots\dots\dots (14)$$

Local contrast of an image is measured by the previous equation.

**Statistical Feature**

The mode value is taken as a statistical feature to be studied in this paper, it represents the most frequent value in the array of the image. It could be expressed as:

$$\text{Mode} = z(i, j) \text{ if } z(i, j) \text{ has a maximum count.} \dots\dots\dots (15)$$

So, first we have to find the count of each pixel intensity, then we choose the maximum count among them.

**Dividing Feature Values into levels**

After the all the pre-studied features are extracted from the MRI sub-segment images, it is necessary to study their variation between the normal and the abnormal segments to discover the changes in their values, and to select the most effected features. But it is not easy to notice the variation of feature values while checking pure numbers. It might be more efficient and easy to divide the feature values into levels according to each feature, and notice the difference between the same feature levels in normal and abnormal images. So the feature values are divided into 3 levels according to their min and max values among all the tested sub segments, these levels are L, representing the Low valued features, M, designating the Medium valued features, and H for the High valued features.

#### 4. RESULTS AND DISCUSSION:

According to the results of the feature values, table 1 below shows the min and max values of the features among all the 789 sub segment images for both normal and abnormal MRI images, and by using some simple calculations they could be divided into 3 levels of (L, M, H).

Calculating the upper limit of the level (L) could be done by the formula:  $((\text{max}-\text{min})/3 + \text{min})$ , While the calculation of the lower limit of the level (H) is obtained from the formula:  $(\text{max} - (\text{max}-\text{min})/3)$ .

Thus the level (L) starts from min to the upper level of (L), while the level (M) starts from the upper level of (L) to the lower level of (H), while the level (H) starts from the lower level of (H) to the max.

mean	variance	stdev	horizontal	vertical	diagonal	entropy	contrast	correlation	Energy	homogeneity	skewness	kurtosis	mode	RMS roughness
min	min	min	min	min	min	min	min	min	min	Min	min	min	min	min
0.278	1.005	1.002	-3.977	0.084	-4.160	0.315	0.004	0.399	0.049	0.646	-3.752	1.221	0.000	1.002
max	max	max	max	max	max	max	max	max	max	Max	max	max	max	max
167.999	10928.750	104.541	3.900	91.570	3.514	7.570	1.459	0.988	0.986	0.998	10.252	113.724	255.000	104.541

L	L	L	L	L	L	L	L	L	L	L	L	L	L	L
0.278	1.005	1.002	-3.977	0.084	-4.160	0.315	0.004	0.399	0.049	0.646	-3.752	1.221	0.000	1.002
56.185	3643.587	35.515	-1.351	30.579	-1.602	2.733	0.489	0.596	0.361	0.763	0.916	38.722	85.000	35.515
M	M	M	M	M	M	M	M	M	M	M	M	M	M	M
56.185	3643.587	35.515	-1.351	30.579	-1.602	2.733	0.489	0.596	0.361	0.763	0.916	38.722	85.000	35.515
112.092	7286.168	70.028	1.275	61.075	0.956	5.151	0.974	0.792	0.674	0.881	5.584	76.223	170.000	70.028
H	H	H	H	H	H	H	H	H	H	H	H	H	H	H
112.092	7286.168	70.028	1.275	61.075	0.956	5.151	0.974	0.792	0.674	0.881	5.584	76.223	170.000	70.028
167.999	10928.750	104.541	3.900	91.570	3.514	7.570	1.459	0.988	0.986	0.998	10.252	113.724	255.000	104.541

**Table 1: Features Extracted from Sub segment MRI Images**

The following two tables shown below describes samples of the sub - segment image feature levels for both normal and abnormal cases, each No. represents a sub segment.

No.	mean	variance	stdev	horizontal	vertical	diagonal	entropy	contrast	correlation	energy	homogeneity	skewness	kurtosis	mode	RMS roughness	Case
1	M	L	L	M	M	M	M	L	M	H	H	L	L	M	L	Normal
2	M	L	L	M	M	M	M	L	M	H	H	L	L	M	L	Normal
3	M	L	L	M	M	M	M	L	H	H	H	L	L	M	L	Normal
4	M	L	L	M	M	M	H	L	H	M	H	L	L	M	L	Normal
5	M	L	L	M	M	M	M	L	H	H	H	L	L	M	L	Normal
6	M	L	L	M	M	M	M	L	H	M	H	L	L	M	L	Normal
7	M	M	M	M	M	H	H	M	H	L	L	M	L	M	M	Normal
8	M	M	H	M	M	M	H	H	H	L	L	L	L	H	H	Normal
9	M	L	L	M	M	M	M	L	M	M	H	L	L	M	L	Normal
10	M	L	L	M	M	M	M	L	M	H	H	L	L	M	L	Normal
11	M	L	L	M	M	M	H	L	H	M	H	L	L	M	L	Normal
12	M	L	L	M	M	M	M	L	M	M	H	L	L	M	L	Normal
13	M	L	L	M	M	M	M	L	M	M	H	L	L	M	L	Normal
14	M	L	L	M	M	M	H	L	H	M	H	L	L	M	L	Normal
15	M	M	M	L	M	M	H	M	H	L	M	M	L	M	M	Normal
16	M	L	L	M	M	M	H	L	H	M	H	L	L	M	L	Normal
17	M	L	L	M	M	M	H	L	H	M	H	L	L	M	L	Normal
18	M	L	L	M	M	M	H	L	M	M	H	L	L	M	L	Normal
19	M	M	H	H	M	H	H	H	H	L	L	L	L	L	H	Normal
20	L	L	M	L	L	M	M	L	H	M	H	M	L	L	M	Normal
21	M	M	H	H	M	M	H	M	H	L	L	L	L	H	H	Normal
22	M	L	L	M	M	M	H	L	H	M	H	L	L	M	L	Normal
23	M	M	H	M	M	H	H	M	H	L	L	L	L	L	H	Normal
24	L	M	M	L	L	M	M	L	H	L	M	M	L	L	M	Normal
25	H	M	M	H	H	M	H	M	H	L	M	L	L	M	M	Normal
26	M	L	L	M	M	M	H	L	M	M	H	L	L	M	L	Normal
27	M	L	L	M	M	M	H	L	M	M	H	L	L	M	L	Normal
28	M	L	L	M	M	M	H	L	M	M	H	L	L	M	L	Normal
29	M	L	L	M	M	M	H	L	H	M	H	L	L	M	L	Normal
30	M	M	M	L	M	M	H	M	H	L	L	L	L	M	M	Normal
31	M	L	L	M	M	M	H	L	H	M	H	L	L	M	L	Normal
32	M	L	L	M	M	M	H	L	H	M	H	L	L	M	L	Normal
33	M	L	L	M	M	M	H	L	M	L	H	M	L	M	L	Normal
34	M	L	L	M	M	M	M	L	M	M	H	L	L	M	L	Normal
35	M	M	M	M	M	H	H	H	H	L	L	L	L	L	M	Normal
36	M	M	H	M	M	M	H	H	H	L	L	L	L	L	H	Normal
37	M	L	L	M	M	M	H	L	M	M	H	M	L	M	L	Normal
38	M	L	L	M	M	M	M	L	M	H	H	L	L	M	L	Normal
39	M	L	L	M	M	M	M	L	L	H	H	L	L	M	L	Normal
40	M	L	L	M	M	M	M	L	H	H	H	L	L	M	L	Normal

Table 2 (A sample of Normal Sub-segment MRI Image Feature Levels)

No.	mean	variance	stdev	horizontal	vertical	diagonal	entropy	contrast	correlation	energy	homogeneity	skewness	kurtosis	mode	RMS roughness	Case
445	M	L	L	M	M	M	M	L	L	H	H	L	L	L	L	Abnormal
446	M	L	L	M	M	M	H	L	H	M	H	L	L	L	L	Abnormal
447	M	L	L	M	M	M	H	L	H	M	H	L	L	M	L	Abnormal
448	M	L	L	M	M	M	H	L	H	M	H	L	L	L	L	Abnormal
449	M	L	L	M	M	M	M	L	H	M	H	L	L	M	L	Abnormal
450	M	L	L	M	M	M	H	L	H	M	H	L	L	L	L	Abnormal
451	M	L	L	M	M	M	H	L	H	M	H	L	L	M	L	Abnormal
452	M	L	L	M	M	M	H	L	H	M	H	M	L	L	L	Abnormal
453	M	L	L	M	M	M	M	L	L	H	H	L	L	L	L	Abnormal
454	M	L	L	M	M	M	H	L	H	M	H	L	L	L	L	Abnormal
455	M	L	L	M	M	M	M	L	H	H	H	L	L	L	L	Abnormal
456	M	L	L	M	M	M	H	L	H	M	H	L	L	L	L	Abnormal
457	M	L	L	M	M	M	H	L	H	M	H	L	L	M	L	Abnormal
458	M	L	L	M	M	M	H	L	H	M	H	L	L	L	L	Abnormal
459	M	L	L	M	M	M	H	L	H	M	H	L	L	M	L	Abnormal
460	M	L	L	M	M	M	H	L	M	H	H	M	L	L	L	Abnormal
461	M	L	L	M	M	M	M	L	M	H	H	L	L	L	L	Abnormal
462	M	L	L	M	M	M	H	L	H	M	H	L	L	M	L	Abnormal
463	M	L	L	M	M	M	M	L	H	H	H	M	L	L	L	Abnormal
464	M	L	L	M	M	M	H	L	H	M	H	L	L	L	L	Abnormal
465	M	L	L	M	M	M	H	L	H	M	H	L	L	M	L	Abnormal
466	M	L	L	M	M	M	H	L	H	M	H	L	L	L	L	Abnormal
467	M	L	L	M	M	M	H	L	H	M	H	L	L	M	L	Abnormal
468	M	L	M	M	L	M	H	L	H	L	H	M	L	L	M	Abnormal
469	M	L	L	M	M	M	H	L	M	H	H	L	L	L	L	Abnormal
470	M	L	L	M	M	M	M	L	L	H	H	L	L	L	L	Abnormal
471	M	L	L	M	M	M	H	L	H	M	H	L	L	L	L	Abnormal
472	M	L	L	M	M	M	H	L	H	H	H	M	L	L	L	Abnormal
473	M	L	L	M	M	M	H	L	H	M	H	L	L	L	L	Abnormal
474	M	L	L	M	M	M	H	L	H	M	H	L	L	M	L	Abnormal
475	M	L	L	M	M	M	H	L	H	M	H	L	L	L	L	Abnormal
476	M	L	L	M	M	M	H	L	M	M	H	L	L	L	L	Abnormal
477	M	L	L	M	M	M	M	L	L	H	H	L	L	L	L	Abnormal
478	M	L	L	M	M	M	H	L	H	M	H	L	L	L	L	Abnormal
479	M	L	L	M	M	M	H	L	H	M	H	L	L	L	L	Abnormal
480	M	L	L	M	M	M	M	L	H	H	H	M	L	L	L	Abnormal
481	M	L	L	M	M	M	M	L	H	H	H	L	L	M	L	Abnormal
482	M	L	L	M	M	M	H	L	H	M	H	L	L	M	L	Abnormal
483	M	L	L	M	M	M	H	L	M	H	H	L	L	L	L	Abnormal
484	M	L	L	M	M	M	M	L	L	H	H	L	L	L	L	Abnormal

Table 3 (A sample of Abnormal Sub-segment MRI Image Feature levels)

**CONCLUSIONS AND FUTURE WORKS**

**Conclusions:**

According to the results of this paper, a statistical study could be gained based on counting each feature level and finding its percentage among the 345 abnormal and the 444 normal cases, as it is shown below in the table 4.

**Table 4 (Features Existence Percentage in Normal and Abnormal Sub – Segment MRI Images)**

mean	variance	stdev	horizontal	vertical	diagonal	entropy	contrast	correlation	energy	homogeneity	skewness	kurtosis	mode	RMS roughness
Normal	Normal	Normal	Normal	Normal	Normal	Normal	Normal	Normal	Normal	Normal	Normal	Normal	Normal	Normal
L	L	L	L	L	L	L	L	L	L	L	L	L	L	L
97	381	256	31	114	25	19	350	2	246	26	334	436	239	256
21.85%	85.81%	57.66%	6.98%	25.68%	5.63%	4.28%	78.83%	0.45%	55.41%	5.86%	75.23%	98.20%	53.83%	57.66%
M	M	M	M	M	M	M	M	M	M	M	M	M	M	M
258	56	162	375	266	367	51	78	72	152	104	102	5	197	162
58.11%	12.61%	36.49%	84.46%	59.91%	82.66%	11.49%	17.57%	16.22%	34.23%	23.42%	22.97%	1.13%	44.37%	36.49%
H	H	H	H	H	H	H	H	H	H	H	H	H	H	H
89	7	26	38	64	52	374	16	370	46	314	8	3	8	26
20.05%	1.58%	5.86%	8.56%	14.41%	11.71%	84.23%	3.60%	83.33%	10.36%	70.72%	1.80%	0.68%	1.80%	5.86%
AbNor.	AbNor.	AbNor.	AbNor.	AbNor.	AbNor.	AbNor.	AbNor.	AbNor.	AbNor.	AbNor.	AbNor.	AbNor.	AbNor.	AbNor.
L	L	L	L	L	L	L	L	L	L	L	L	L	L	L
29	342	307	7	29	4	0	340	22	90	0	293	344	125	307
8.41%	99.13%	88.99%	2.03%	8.41%	1.16%	0.00%	98.55%	6.38%	26.09%	0.00%	84.93%	99.71%	36.23%	88.99%
M	M	M	M	M	M	M	M	M	M	M	M	M	M	M
206	3	38	329	232	328	60	4	95	178	21	51	1	218	38
59.71%	0.87%	11.01%	95.36%	67.25%	95.07%	17.39%	1.16%	27.54%	51.59%	6.09%	14.78%	0.29%	63.19%	11.01%
H	H	H	H	H	H	H	H	H	H	H	H	H	H	H
110	0	0	9	84	13	285	1	228	77	324	1	0	2	0
31.88%	0.00%	0.00%	2.61%	24.35%	3.77%	82.61%	0.29%	66.09%	22.32%	93.91%	0.29%	0.00%	0.58%	0.00%

From checking the table, it would be easy to discover that some features are really affected by the existence of tumors, the following conclusions could be detected:

- 1- In normal cases, the mean value feature has a level of (L) with a percentage of about 22% of existence, and a level of (M) with a percentage of about 58% and an (H) level of 20%, while in abnormal cases the level (L) drops from 22% to be 8.4%, and the level (M) becomes about 60% which is near to its value in the normal cases, but the (H) level increases from 20% to about 32%. Thus it is obvious that the mean feature with high values (H) is more probable to exist in abnormal cases.
- 2- The standard deviation and the variance have an existence percentage of 0% in the level (H) with abnormal cases which means that they have no high values if the MRI sub segment image is infected. But the variance differs from the standard deviation by having larger values of percentage at low levels (L) from the standard deviation.
- 3- In normal cases, the vertical feature has its minimum percentage of existence in the level (H) which is 14%, this is changed in abnormal cases to the level (L) with 8.4%.
- 4- Another histogram feature, the entropy, has no small values (L=0%) if the MRI sub segment is abnormal.
- 5- The feature of energy changes from 55% as low level values in normal images to only 26% in abnormal images, and it has its maximum percentage at (M) level if the image is abnormal.
- 6- The homogeneity feature has no existence at low levels if the image is abnormal, on the contrast of the kurtosis feature which has no high values in abnormal images.
- 7- For the mode feature, if we get its value in the medium range, we first assume to be abnormal, because it has a percentage of about 63% at this level, while this feature has its maximum percentage of about 53% in the normal images at the low leveled values.
- 8- The RMS roughness has no existence at high values if the image is abnormal.
- 9- The features of (horizontal, diagonal, contrast, correlation, skewness) didn't changed in their percentage of existence from normal to abnormal images, so we can consider them passive features according to this type of study.
- 10- According to this paper, ranking the features is related to their affecting toward the abnormal MRI image sub segments. The highest rank will be for the features of (mean, energy and the mode) features as it is discovered from table 4, then the features (variance, standard deviation, entropy, vertical, homogeneity, kurtosis and RMS roughness), finally the features (horizontal, diagonal, contrast, correlation, skewness) which could be neglected due to their infectivity toward normal and abnormal changes in MRI images.

### **FUTURE WORKS**

More studies could be applied based on the results of this paper, especially the field of choosing other types of features. Different medical imaging techniques could be used like the CT-Scan or else. Also other parts of the human body could be diagnosed, feature extracted and studied.

Real time processing techniques could be connected to this type of diagnosing method, connecting medical imaging techniques to computers having application of medical diagnosing will help to get immediate reports about the patients situation.

### **REFERENCES**

- [1]. Xiaobing LI, "Automatic image segmentation based on level set approach: application to brain tumor segmentation in MR images", Ph.D. thesis, University of Reims Champagne-Ardenne, Graduate School Health Science Technology, France, 22/12/2009.
- [2]. D.N. Louis, H. Ohgaki, O. D. Wiestler, W. K. Cavenee, P. C. Burger, A. Jouvet, B. W. Scheithauer and P. Kleihues, "The 2007 WHO Classification of Tumours of the Central Nervous System", International Agency for Research on Cancer (IARC), Lyon, France, 2007.
- [3]. Policy Analysis and Public Affairs, "Medical Imaging in Cancer Care: Charting The Progress", US Oncology and National Electrical Manufacturers Association (NEMA), accessed on January 2013. [http://www.healthcare.philips.com/pwc\\_hc/us\\_en/about/Reimbursement/assets/docs/cancer\\_white\\_paper.pdf](http://www.healthcare.philips.com/pwc_hc/us_en/about/Reimbursement/assets/docs/cancer_white_paper.pdf).
- [4]. Ahlam Fadhil Mahmood, Ameen Mohammed Abd-Alsalam, "Automatic Brain MRI Slices Classification Using Hybrid Technique", AL Rafdain Engineering Journal, ISSN: 18130526, Vol. 22, No. 3, PP. 198-212, Mosul University, Iraq, 2014.
- [5]. Ameen Mohammed Abd-Alsalam, "Brain Tumor Detection and Tissue Segmentation from MRI Images using a Hybrid Technique", M.Sc. thesis, Mosul University, Iraq, 2013.
- [6]. Z. Nan, "Feature Selection based Segmentation of Multi-Source Images: Application to Brain Tumor Segmentation in Multi-Sequence MRI", Ph.D. thesis doctoral training: information sciences, devices and systems, The National Institute of Applied Sciences in Lyon, 12 September, 2011.
- [7]. K. D. Kharatl, P. P. Kulkarni and M.B. Nagori, "Brain Tumor Classification Using Neural Network Based Methods", International Journal of Computer Science and Informatics, ISSN: 2231-5292, Vol.1, Issue 4, PP.85-90, 2012.

- [8]. S. J. Hussain, T. S. Savithri and P.V. Devi, "Segmentation of Tissues in Brain MRI Images using Dynamic Neuro-Fuzzy Technique", *International Journal of Soft Computing and Engineering (IJSCE)*, ISSN: 2231-2307, Volume-1, Issue-6, January 2012.
- [9]. D. K. Kole, A. Halder, "Automatic Brain Tumor Detection and Isolation of Tumor Cells from MRI Images", *International Journal of Computer Applications*, ISSN: 0975-8887, Vol. 39, Issue 16, PP. 26-30, February 2012.
- [10]. Q. Ain, G. Latif, S. B. Kazmi, M. A. Jaffar And A. M. Mirza, "Classification and Segmentation of Brain Tumor using Texture Analysis", *AIKED'10 Proceedings of the 9th WSEAS international conference on Artificial intelligence, knowledge engineering and data bases*, Cambridge, UK, February 20-22, 2011.
- [11]. D. Mitre, M. Socaciu, R. Badea and A. Golea, "Texture Based Characterization and Automatic Diagnosis of the Abdominal Tumors from Ultrasound Images using Third Order GLCM Features", *4th International Congress on Image and Signal Processing*, Vol. 3, PP. 1558 – 1562, TBD Shanghai, China, 15-17 October 2011.
- [12]. K. M. Iftakharuddin, S. Ahmed and J. Hossen, "Multiresolution texture models for brain tumor segmentation in MRI", *33rd Annual International Conference of the IEEE EMBS*, Boston, Massachusetts USA, ISSN: 1557170X, PP. 6985- 6988, August 30 - September 3, 2011.
- [13]. M. Kumar and K. K. Mehta, "A Texture based Tumor detection and automatic Segmentation using Seeded Region Growing Method", *International Journal of Computer Technology and Applications*, ISSN: 2229-6093, Vol. 2, Issue 4, PP. 855-859, August 2011.
- [14]. N. Just, "Improving tumor heterogeneity MRI assessment with histograms", *British Journal of Cancer (BJC)*, ISSN: 0007-0920, Vol. 111(12), PP. 2205–2213, 2014 Dec 9.
- [15]. Adegoke, B.O, Ola, B.O., and Omotayo, M.E, "Review of Feature Selection Methods in Medical Image Processing", *IOSR Journal of Engineering (IOSRJEN)*, Vol. 04, Issue 01, ISSN (Print): 2278-8719, ISSN (Online): 2250-3021, PP. 01-05, January 2014.
- [16]. Saurabh Shah, N.C. Chauhan, "Classification of Brain MRI Images using Computational Intelligent Techniques", *International Journal of Computer Applications*, ISSN: 0975-8887, Vol. 24, No.14, August 2015.
- [17]. Mr. R. Kishore, "AN EFFECTIVE AND EFFICIENT FEATURE SELECTION METHOD FOR LUNG CANCER DETECTION", *International journal of Computer Science & Information Technology (IJCSIT)*, ISSN: 2074-9007 (Print), ISSN: 2074-9015 (Online), Vol. 7, No. 4, August 2015.
- [18]. V. Sheejakumari and Sankara Gomathi, "Brain tumor detection from MRI images using histon based segmentation and modified neural network", *Biomedical Research*, Special Issue: S1-S9, ISSN: 0970-938X, 2016.
- [19]. K. Muthukarpagam and Dr. P. Eswaran, "Feature Extraction Based Brain Tumor Detection in MRI Images", *International Journal of Advanced Research Trends in Engineering and Technology (IJARTET)*, Vol. 3, Special Issue 20, ISSN: 2394-3777 (Print), ISSN 2394-3785 (Online), April 2016.
- [20]. R. C. Gonzalez, Richard E. Woods, "Digital Image Processing", 2nd edition, Prentice Hall, 2002.
- [21]. Robert A. Schowengerdt, "Remote Sensing, Models and Methods for Image Processing", 2nd edition, Academic Press, 1997.
- [22]. K. Boussu, et al., "Roughness and hydrophobicity studies of nanofiltration membranes using different modes of AFM", *Journal of Colloid and Interface Science (JCIS)*, ISSN: 0021-9797, V. 286, Issue 2, pp. 632–638, 15 June 2005.
- [23]. E. Brannock, "Using the Discrete Wavelet Transform to Haar'd Code: A blind Digital Watermark", Ph.D. Dissertation in the College of Arts and Science, Georgia State University, 2009.